



Research article

Mathematical modeling and optimal control of tuberculosis spread among smokers with case detection

Cicik Alfiniyah^{1,*}, Wanwha Sonia Putri Artha Soetjianto¹, Ahmadin¹, Muhamad Hifzhudin Noor Aziz² and Siti Maisharah Sheikh Ghadzi³

¹ Department of Mathematics, Faculty of Science and Technology, Universitas Airlangga, Indonesia

² Institute of Mathematical Sciences, Faculty of Science, Universiti Malaya, Malaysia

³ School of Pharmaceutical Sciences, Universiti Sains Malaysia, Malaysia

* **Correspondence:** Email: cicik-a@fst.unair.ac.id.

Abstract: Tuberculosis (TB) remains one of deadly infectious diseases worldwide. Smoking habits are a significant factor that can increase TB transmission rates, as smokers are more susceptible to contracting TB than nonsmokers. Therefore, a control strategy that focused on minimizing TB transmission among smokers was essential. The control of TB transmission was evaluated based on the case detection rate. Undetected TB cases often resulted from economic challenges, low awareness, negative stigma toward TB patients, and health system delay (HSD). In this study, we developed a mathematical model that captured the dynamics of TB transmission specifically among smokers, incorporating the effects of case detection. Our innovative approach lied in the integration of smoking behavior as a key factor in TB transmission dynamics, which has been underexplored in previous models. We analyzed the existence and stability of the TB model equilibrium based on the basic reproduction number. Additionally, parameter sensitivity analysis was conducted to identify the most influential factors in the spread of the disease. Furthermore, this study investigated the effectiveness of various control strategies, including social distancing for smokers, TB screening in high-risk populations, and TB treatment in low-income communities. By employing the Pontryagin maximum principle, we solved optimal control problems to determine the most effective combination of interventions. Simulation results demonstrated that a targeted combination of control measures can effectively reduce the number of TB-infected individuals.

Keywords: tuberculosis; mathematical model; sensitivity analysis; optimal control; smokers; case detection rate

Mathematics Subject Classification: 34A34, 34A45, 92C60, 92D30, 93C15

1. Introduction

Tuberculosis (TB), caused by the bacterium *Mycobacterium tuberculosis*, spreads through the air and primarily affects the lungs, although it can also affect other parts of the body [1]. Most commonly, TB damages the lungs, leading to symptoms such as chronic cough, chest pain, and coughing up blood, which result in breathing difficulties [2]. Transmission occurs when individuals with active TB release bacteria into the air through actions such as coughing, sneezing, or talking [3]. These airborne bacteria can be inhaled by others, leading to new infections. TB infection can result in either latent TB, where the bacteria remain inactive and the individual is not contagious, or active TB, where the bacteria are active and the individual can spread the disease to others [1].

Individuals with latent TB do not exhibit symptoms and cannot transmit the infection, but they carry a risk of developing active TB, particularly if their immune system becomes weakened [4]. In contrast, those with active TB typically exhibit symptoms that may include prolonged cough, fever, night sweats, and weight loss. Effective treatment requires a prolonged course of antibiotics, and the management of TB is further complicated by the emergence of drug-resistant strains of the bacterium [5]. Prevention strategies include vaccination with the *Bacillus Calmette-Guérin* (BCG) vaccine, early detection through screening programs, and ensuring adherence to treatment protocols to reduce transmission and prevent the development of drug resistance [6].

TB is the second most deadly infectious disease in the world. The highest number of TB cases are reported in countries such as India, China, Indonesia, Philippines, Pakistan, Nigeria, Bangladesh, and South Africa [1]. The impact of TB in such countries is multifaceted. Economically, TB can lead to significant healthcare costs and loss of productivity due to illness and death. Patients often face prolonged treatment regimens that can strain personal and public health resources. Socially, TB patients frequently encounter stigma and social exclusion [1], which can deter individuals from seeking timely medical intervention and support. One of the significant factors contributing to the high transmission of TB in these communities is smoking habits. Smokers have a risk of dying from and transmitting TB that is two times higher than that of nonsmokers [7, 8]. Mathematical modeling predicts that smoking will result in 18 million TB events and 40 million deaths from TB worldwide between 2010 and 2050 [9].

Efforts to control TB in these high-burden countries involve comprehensive strategies that address both medical and social challenges. This includes widespread TB screening and vaccination programs [10], public health campaigns to reduce smoking, and educational initiatives to reduce stigma associated with the disease [6]. Additionally, strengthening healthcare infrastructure and ensuring access to effective treatments are crucial to managing and reducing TB transmission. The fight against TB is further complicated by the rise of multidrug-resistant TB (MDR-TB), which requires more complex and expensive treatment protocols, emphasizing the need for sustained global health efforts and funding [11].

Mathematical models have significantly contributed to understanding TB transmission dynamics and developing control strategies. Various models have been established to better comprehend the disease's dynamics and the effectiveness of interventions (see, for example, [12–14] and references therein). Liu and Zhang [15] developed a model that considers both vaccinated and treated populations, providing insights into how vaccination and treatment strategies can influence TB dynamics. Ullah et al. [16] discussed a model that accounts for individuals recovering after treatment,

highlighting the importance of post-treatment recovery phases in controlling the spread of TB. Khan et al. [17] explored TB transmission dynamics in a specific region, Khyber Pakhtunkhwa, Pakistan, illustrating the regional variations in TB spread and the necessity for localized intervention strategies. Furthermore, the mathematical model of the spread of TB among smokers demonstrates that the level of smoking recruitment significantly affects the expected number of secondary infections, emphasizing the impact of smoking on TB transmission dynamics [7]. Researchers have also proposed optimal control strategies to assess intervention effectiveness, incorporating factors such as vaccination, treatment, and prevention efforts [18–20].

This research introduces a novel approach by integrating smoking behavior and case detection into a mathematical model of TB transmission, specifically focusing on high-smoking populations. Unlike previous models that treated smoking as a secondary factor, our model centers on smoking habits as a core element of TB transmission dynamics. The innovation lies in introducing control strategies that target smoking behavior, such as social distancing among smokers, specialized TB screening, and treatment in high-risk communities. We employ optimal control theory to identify the most effective interventions, emphasizing specific strategies to reduce TB transmission rates among smokers. Enhancing case detection rates (CDR) is critical, as the WHO reported that 39.43% of TB cases were undetected globally in 2021, causing a significant risk for further spread. Improving CDR through thorough examinations and financial support for treatment, particularly in low-income communities, can encourage TB sufferers to seek and complete medical care. Our model builds on existing TB transmission frameworks [21] by incorporating these control variables to minimize latent TB cases and both detected and undetected active TB cases.

This paper is structured as follows: Section 2 presents the formulation of the TB model in the smoker population. Section 3 covers basic properties, stability analysis, and parameter sensitivity analysis of the model. Sections 4 and 5 discuss optimal control formulation and numerical simulations, respectively. Finally, Section 6 summarizes the research conclusions.

2. Formulation of a TB model in smoker population

In this section, a mathematical model of the spread of TB among smokers with case detection is formulated. The assumptions used for the model construction are as follows:

- (1) Infection with Mycobacterium TB in the human body occurs slowly.
- (2) The BCG vaccine does not provide complete protection against Mycobacterium TB infection.
- (3) TB patients cannot recover without medical TB treatment.
- (4) Medical TB treatment is not always successful.

The human population is divided into seven compartments, which are the nonsmoker population (S), the smoker population (M), the vaccinated population (V), the latent TB population (E), undetected active TB population (I_1), detected active TB population (I_2), and the population who have recovered from TB (T). Based on the assumptions, we can set up the transmission diagram that is shown in Figure 1.

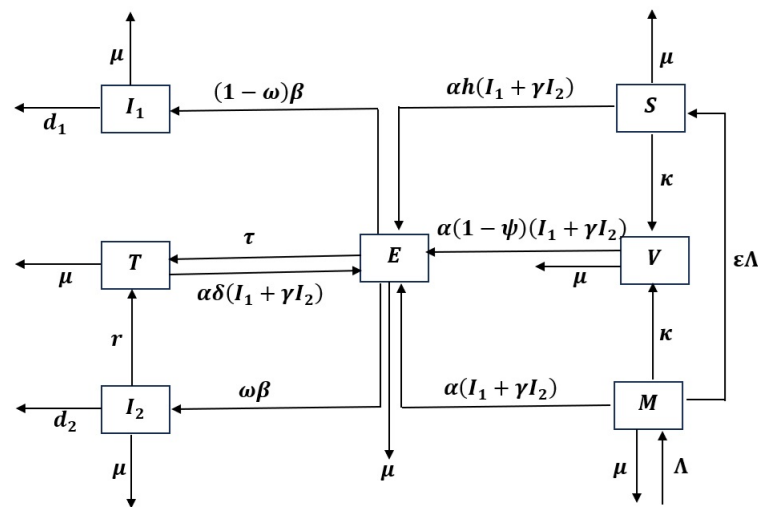


Figure 1. Transmission diagram. Mathematical model of the spread of TB disease among smokers with case detection.

The defining parameters can be seen in Table 1, which are assumed constant and nonnegative.

Table 1. Parameters. Description of parameters in the model of the spread of TB disease among smokers with case detection.

| Par | Description |
|---------------|--|
| Λ | Smoking recruitment rate |
| ε | Proportion of individuals who refuse or ignore smoking recruitment |
| α | TB disease transmission rate |
| h | The probability that the nonsmoker population can be infected by <i>Mycobacterium tuberculosis</i> |
| γ | The probability of TB transmission by a detected active TB population |
| μ | Natural death rate |
| κ | BCG vaccination rates |
| ψ | BCG vaccine effectiveness |
| ω | The proportion of the latent TB population that develops active TB that is detected |
| d_1 | Death rate in an undetected active TB population |
| β | The rate of development of a population of latent TB to active TB |
| d_2 | Death rate in a detected active TB population |
| r | Medical treatment rate in the detected active TB population |
| δ | TB reinfection rate in the population that has recovered from TB |
| τ | Treatment rates in the medically latent TB population |

From the diagram in Figure 1, transmission models can be formulated as follows:

$$\frac{dS}{dt} = \varepsilon\Lambda - \alpha h S (I_1 + \gamma I_2) - (\mu + \kappa) S, \quad (2.1)$$

$$\frac{dM}{dt} = \Lambda - \varepsilon\Lambda - \alpha M (I_1 + \gamma I_2) - (\mu + \kappa) M, \quad (2.2)$$

$$\frac{dV}{dt} = \kappa (S + M) - \alpha (1 - \psi) V (I_1 + \gamma I_2) - \mu V, \quad (2.3)$$

$$\frac{dE}{dt} = \alpha (I_1 + \gamma I_2) (hS + M + (1 - \psi) V + \delta T) - (\tau + \beta + \mu) E, \quad (2.4)$$

$$\frac{dI_1}{dt} = (1 - \omega)\beta E - (\mu + d_1)I_1, \quad (2.5)$$

$$\frac{dI_2}{dt} = \omega\beta E - (\mu + d_2 + r)I_2, \quad (2.6)$$

$$\frac{dT}{dt} = rI_2 + \tau E - \delta\alpha T (I_1 + \gamma I_2) - \mu T. \quad (2.7)$$

The non-endemic equilibrium point for the mathematical model of the spread of TB disease among smokers with case detection occurs if there are no active TB sufferers in a population, either detected or undetected. Suppose the non-endemic equilibrium point for the mathematical model of the spread of TB disease with case detection is expressed as L_0 . Substituting

$$I_1 = I_2 = 0$$

into (2.1)–(2.7) will get

$$L_0 = (S, M, V, E, I_1, I_2, T) = \left(\frac{\varepsilon\Lambda}{\mu + \kappa}, \frac{\Lambda - \varepsilon\Lambda}{\mu + \kappa}, \frac{\kappa\Lambda}{\mu(\mu + \kappa)}, 0, 0, 0, 0 \right).$$

Next, we will determine the basic reproduction number (R_0) which has the important role in the disease modeling [22, 23]. The basic reproduction number (R_0) can be computed using the next generation matrix on the TB models (2.1)–(2.7). Consider the infected compartments are L, I, and T. Using the approach in [24], the matrices F and V at disease free equilibrium are given as follows:

$$F = \begin{pmatrix} 0 & \frac{\alpha\Lambda(h\varepsilon\mu + \mu - \mu\varepsilon + \kappa - \kappa\psi)}{\mu(\mu + \kappa)} & \frac{\alpha\gamma\Lambda(h\varepsilon\mu + \mu - \mu\varepsilon + \kappa - \kappa\psi)}{\mu(\mu + \kappa)} \\ 0 & 0 & 0 \\ 0 & 0 & 0 \end{pmatrix}$$

and

$$V = \begin{pmatrix} \tau + \beta + \mu & 0 & 0 \\ -(1 - \omega)\beta & \mu + d_1 & 0 \\ -\omega\beta & 0 & \mu + d_2 + r \end{pmatrix}.$$

The basic reproduction number (R_0) of the model is obtained through the spectral radius of the matrix

$$R_0 = \rho(FV^{-1}),$$

which is given by

$$R_0 = \frac{\alpha\Lambda\beta(h\varepsilon\mu + \mu(1 - \varepsilon) + \kappa(1 - \psi))((\mu + d_2 + r)(1 - \omega) + \gamma\omega(\mu + d_1))}{\mu(\mu + \kappa)(\tau + \beta + \mu)(\mu + d_1)(\mu + d_2 + r)}.$$

Furthermore, the endemic equilibrium point for the mathematical model of the spread of TB disease among smokers with case detection is obtained when there are active TB sufferers in a population. Suppose the endemic equilibrium point for the mathematical model of the spread of TB disease with case detection is expressed as L_1 . Substituting $I_1 \neq 0$ and $I_2 \neq 0$ into Eqs (2.1)–(2.7) will get

$$L_1 = (S^*, M^*, V^*, E^*, I_1^*, I_2^*, T^*),$$

where

$$\begin{aligned}
 S^* &= \frac{\varepsilon\Lambda(\mu + d_1)(\mu + d_2 + r)}{\alpha h\beta E^* ((1 - \omega)(\mu + d_2 + r) + \gamma\omega(\mu + d_1)) + (\mu + \kappa)(\mu + d_1)(\mu + d_2 + r)}, \\
 M^* &= \frac{\Lambda(1 - \varepsilon)(\mu + d_1)(\mu + d_2 + r)}{\alpha\beta E^* ((1 - \omega)(\mu + d_2 + r) + \gamma\omega(\mu + d_1)) + (\mu + \kappa)(\mu + d_1)(\mu + d_2 + r)}, \\
 V^* &= \frac{\kappa(S^* + M^*)}{\alpha(1 - \psi)(I_1^* + \gamma I_2^*) + \mu}, \\
 I_1^* &= \frac{(1 - \omega)\beta E^*}{(\mu + d_1)}, \\
 I_2^* &= \frac{\omega\beta E^*}{\mu + d_2 + r}, \\
 T^* &= \frac{(\mu + d_1)(r\omega\beta + \tau(\mu + d_2 + r))}{\delta\alpha\beta E^* ((1 - \omega)(\mu + d_2 + r) + \gamma\omega(\mu + d_1)) + \mu(\mu + d_1)(\mu + d_2 + r)},
 \end{aligned}$$

and $E^* > 0$ if $R_0 > 1$.

Local stability analysis of the equilibrium point is crucial for understanding the system's behavior as it approaches equilibrium. In our study, we modeled the spread of TB among smokers, incorporating case detection, and using a system of nonlinear differential equations. To analyze the stability of the equilibrium points, we linearized the system around these points using the Jacobian matrix. The local stability of an equilibrium point is determined by calculating the eigenvalues of the Jacobian matrix.

We specifically examined the stability of the non-endemic equilibrium point by substituting L_0 into the Jacobian matrix. The non-endemic equilibrium point is asymptotically stable if all the eigenvalues of the Jacobian matrix have negative real parts. This condition ensures that any small perturbations around the equilibrium point will decay over time, causing the system to return to equilibrium. The condition is met if

$$\begin{aligned}
 R_0 &= \frac{\beta\alpha\Lambda(h\varepsilon\mu + \mu(1 - \varepsilon) + (1 + \psi)\kappa)((1 - \omega)(\mu + d_2 + r) + \omega\gamma(\mu + d_1))}{(\tau + \beta + \mu)(\mu + d_1)(\mu + d_2 + r)\mu(\mu + \kappa)} < 1, \\
 R_1 &= \frac{\beta\alpha\Lambda(h\varepsilon\mu + \mu(1 - \varepsilon) + (1 + \psi)\kappa)((1 - \omega) + \omega\gamma)}{\mu(\mu + \kappa)((\mu + d_1)(\mu + d_2 + r) + (\tau + \beta + \mu)(\mu + d_2 + r) + (\tau + \beta + \mu)(\mu + d_1))} < 1, \\
 R_2 &= \frac{\beta\alpha\Lambda(h\varepsilon\mu + \mu(1 - \varepsilon) + (1 + \psi)\kappa)}{((\mu + d_2 + r) + (\mu + d_1) + (\tau + \beta + \mu) + (\mu + d_1 + \tau + \beta + \mu)(\tau + \beta + \mu)(\mu + d_1))} \\
 &\quad \times \frac{(\omega\gamma(\mu + d_2 + r + \tau + \beta + \mu) + (1 - \omega)(\mu + d_1 + \tau + \beta + \mu))}{((\mu + d_1)(\mu + d_2 + r) + (\tau + \beta + \mu)(\mu + d_2 + r))\mu(\mu + \kappa)} < 1.
 \end{aligned}$$

Because $R_1 < R_0$ and $R_2 < R_0$, it can be concluded that the non-endemic equilibrium point (L_0) is asymptotically stable if $R_0 < 1$.

The stability of the endemic equilibrium point of the mathematical model for the spread of TB disease among smokers, incorporating case detection, was analyzed by substituting the endemic equilibrium point L_1 into the Jacobian matrix. We faced challenges due to our model yielding a seventh-degree polynomial, which makes a detailed analytical analysis of the endemic equilibrium extremely difficult. However, we can explore the possibility of analyzing the endemic equilibrium by referring to Abboubakar's work [25], which may provide insights for future work in another case. Due to the complexity of analytically determining the eigenvalues of the Jacobian matrix for this

nonlinear system, we employed numerical simulations to assess the stability of the endemic equilibrium points. These simulations involved the use of phase planes to visualize the system's trajectories and observe their behavior around the equilibrium point. By setting specific parameter values and initial conditions, we were able to simulate the dynamics of the TB spread model.

The parameter values and initial conditions used in these simulations are detailed in Tables 2 and 3. We selected parameter values based on established references rather than estimating them from real data to ensure the accuracy and reliability of our model. By using values that have been validated and widely accepted in the literature, we can confidently build a model that accurately reflects the dynamics of TB spread among smokers. Through this approach, we gained a deeper understanding of the stability characteristics of the endemic equilibrium in the context of TB spread among smokers.

Table 2. Parameter value in a mathematical model of the spread of TB disease among smokers with case detection.

| Parameter | Unit | Value | Source |
|---------------|-------------|-------|---------|
| Λ | people/time | 50 | Assumed |
| ε | - | 0,45 | Assumed |
| α | 1/time | 0,7 | [26] |
| h | - | 0,9 | Assumed |
| γ | - | 0,5 | [21] |
| μ | 1/time | 0,85 | [21] |
| κ | 1/time | 0,65 | [26] |
| ψ | - | 0,50 | [26] |
| ω | - | 0,11 | [21] |
| d_1 | 1/time | 0,365 | [21] |
| d_2 | 1/time | 0,22 | [21] |
| r | 1/time | 1,5 | [21] |
| δ | 1/time | 1,5 | [21] |
| τ | 1/time | 0,06 | [7] |
| β | 1/time | 0,17 | [7] |

Table 3. Initial values of the mathematical model of the spread of TB among smokers with case detection for endemic conditions

| Variable | Initial value | | |
|----------|---------------|----|----|
| | 1 | 2 | 3 |
| $S(0)$ | 16 | 35 | 63 |
| $M(0)$ | 20 | 50 | 70 |
| $V(0)$ | 30 | 45 | 55 |
| $E(0)$ | 35 | 40 | 60 |
| $I_1(0)$ | 11 | 34 | 48 |
| $I_2(0)$ | 10 | 20 | 35 |
| $T(0)$ | 9 | 15 | 25 |

The simulation was carried out over a time span from $t = 0$ to $t = 1000$. Three distinct initial values were used in the simulation to assess the convergence of solutions from each starting point. This approach aimed to determine whether the system consistently converges to the endemic equilibrium point regardless of initial conditions, thereby providing a robust validation of the model's

stability. Each set of initial values represents different starting conditions for the compartments in the TB spread model, allowing us to observe how the system evolves over time from various initial states. The behavior of the trajectories from these initial values helps to illustrate the stability and potential attractor properties of the endemic equilibrium point.

Based on Figure 2, it is seen that at the moment when the initial value is given, the population graph tends to converge to a single point

$$(M; I_1) = (5.56; 4.74)$$

which is the point of the endemic equilibrium point

$$L_1 = (4.82; 5.7; 2.62; 39.22; 4.88; 0.28; 0.45).$$

In addition, based on the parameter values in Table 2, the value $R_0 = 3, 70 > 1$.

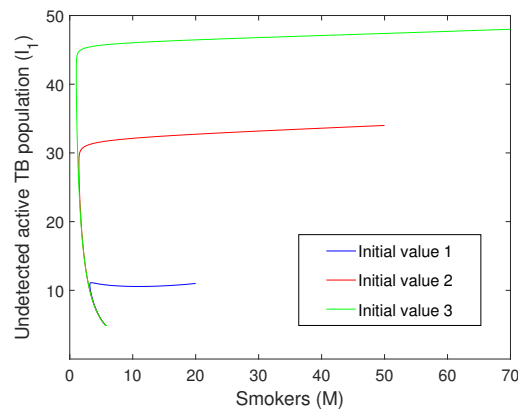


Figure 2. The phase field of smokers and undetected active TB population.

3. Parameter sensitivity analysis

The sensitivity analysis of parameters aims to identify which parameters significantly influence the stability conditions of both the non-endemic and endemic equilibrium points. The magnitude of the parameter's influence is determined based on the sensitivity index (e_m). The sensitivity index (e_m) for parameter m , according to Chitnis et al. [27], is formulated as follows:

$$e_m = \left(\frac{\partial R_0}{\partial m} \right) \frac{m}{R_0}. \quad (3.1)$$

The stability of the non-endemic and endemic equilibrium points in the mathematical model of TB spread among smokers with case detection is determined by the value of R_0 . There are 14 parameters that affect the value of R_0 , namely $\alpha, \Lambda, \beta, h, \epsilon, \mu, \kappa, \psi, \omega, \gamma, d_2, r, d_1$, and τ . The sensitivity indices of these parameters and the relationship between changes in these parameters and the resulting changes in R_0 are presented in the Table 4.

Table 4. Index of parameter sensitivity.

| Parameter (p) | Sensitivity index | $R_0 = 3,7031$ | | | |
|-------------------|-------------------|----------------|-----------|-----------|------------|
| | | $p - 10\%$ | $p - 5\%$ | $p + 5\%$ | $p + 10\%$ |
| α | 1 | 3.3328 | 3.5180 | 3.8883 | 4.0734 |
| Λ | 1 | 3.3328 | 3.5180 | 3.8883 | 4.0734 |
| β | 0,8426 | 3.3861 | 3.5459 | 3.8579 | 4.0103 |
| h | 0,3028 | 3.5910 | 3.6471 | 3.7592 | 3.8153 |
| ε | -0,0336 | 3.7156 | 3.7094 | 3.6969 | 3.6907 |
| μ | -2,3287 | 4.7219 | 4.1707 | 3.3038 | 2.9605 |
| d_1 | -0,2919 | 3.8146 | 3.7580 | 3.6499 | 3.5982 |
| κ | -0,1474 | 3.7602 | 3.7310 | 3.6764 | 3.6508 |
| ψ | -0,2859 | 3.8090 | 3.7561 | 3.6502 | 3.5972 |
| ω | -0,0917 | 3.7371 | 3.7201 | 3.6861 | 3.6692 |
| γ | 0,0284 | 3.6926 | 3.6979 | 3.7084 | 3.7136 |
| d_2 | -0,0024 | 3.7040 | 3.7036 | 3.7027 | 3.7022 |
| r | -0,0166 | 3.7096 | 3.7063 | 3.7001 | 3.6973 |
| τ | -0,0556 | 3.7238 | 3.7134 | 3.6929 | 3.6827 |

A sensitivity index that has a positive value indicates that an increase in the parameter's value leads to an increase in R_0 . Conversely, a sensitivity index with a negative value implies that an increase in the parameter's value results in a decrease in R_0 . Understanding these relationships is crucial for identifying which parameters most significantly impact the basic reproduction number and, consequently, the potential for disease spread. For example, $\alpha = 1$ means that if the value of α decreases (or increases) by 10%, R_0 will decrease (or increase) by 10% as well. Similarly, $\beta = 0.8426$ suggests that a 10% decrease (or increase) in β leads to an 8.4% decrease (or increase) in R_0 . On the other hand, a negative sensitivity index means that an increase in the parameter value causes R_0 to decrease. For instance, $\psi = -0.2859$ indicates that if ψ decreases (or increases) by 10%, R_0 will increase (or decrease) by 2.8%. This analysis applies to parameters $\alpha, \Lambda, \beta, h, \varepsilon, \mu, \kappa, \psi, \omega, \gamma, d_2, r, d_1,$ and τ .

Understanding the sensitivity index of these parameters is crucial for predicting how changes in various factors influence the spread of TB. Parameters like α and β are directly linked to smoking behavior, where an increase in α (indicating a higher rate of progression from latent to active TB) and β (indicating higher transmission rates) directly increases R_0 , the basic reproduction number. This increase signifies a greater potential for TB spread within the population, making it important to control smoking to reduce these parameters.

On the other hand, parameter such as ψ , which represents vaccine effectiveness, has a negative sensitivity index. This suggests that improving these interventions (increasing ψ) reduces R_0 , thereby curbing the spread of TB. The detailed sensitivity analysis of these parameters not only highlights the impact of smoking behavior on TB dynamics but also underscores the importance of targeted interventions to manage and control the disease effectively. By strategically adjusting these parameters, control strategies can be optimized to achieve a significant reduction in TB transmission, particularly in populations with high smoking rates.

The numerical simulation results for the sensitivity of parameters α and ψ to R_0 (presented in Figure 3) align with the observed effects of smoking behavior on the spread of TB, as illustrated in the earlier figures. Specifically, the parameter α represents the rate at which latent TB progresses to active

TB, and as shown, increasing α raises R_0 , underscoring the critical role of smoking in facilitating the transition from latent to active TB. This is consistent with the earlier findings, where higher smoking intensity led to an increased latent TB population, which in turn can elevate the risk of these cases becoming active, thereby driving up the basic reproduction number R_0 and accelerating TB spread.

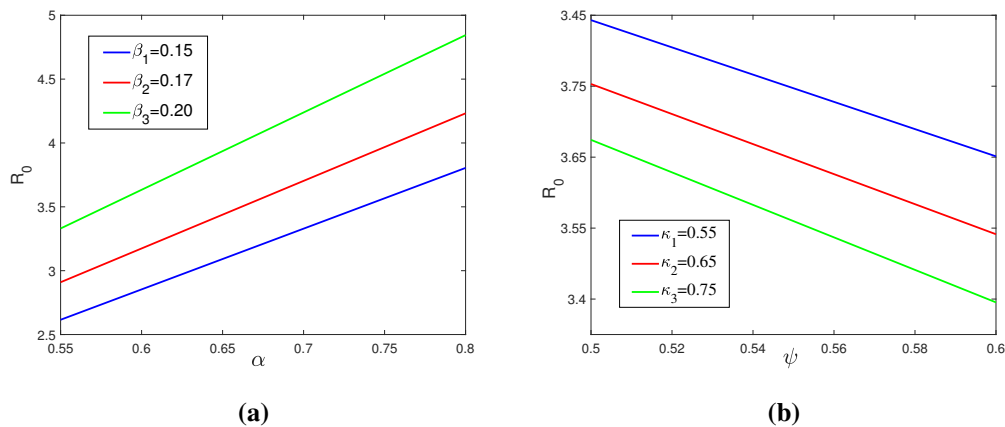


Figure 3. Parameters sensitivity analysis for α and ψ .

Focusing on the parameters α and β , both are crucial in demonstrating how smoking behavior influences the spread of TB. Understanding the interplay between these parameters and smoking behavior is essential for developing strategies that can reduce R_0 , control TB spread, and ultimately lead to the eradication of the disease, particularly in smoker populations. The parameter α , representing the rate at which latent TB progresses to active TB, is directly affected by smoking habits. As seen in the numerical simulations Figure 3a, an increase in α leads to a higher R_0 , indicating that smoking accelerates the progression of latent TB to active TB, thereby increasing the potential for TB transmission within a population.

The Figure 4 presented the influence of smoking behavior on the spread of TB, focusing on different populations within the disease dynamics.

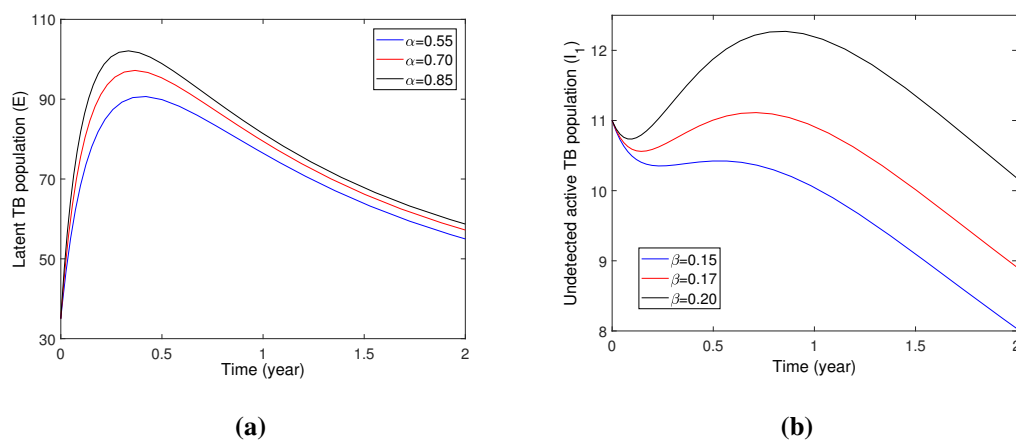


Figure 4. The effect of smoking habits on (a) exposed and (b) undetected active TB population. All parameter values are in Table 2.

In the Figure 4a, the impact of varying levels of smoking intensity (represented by α values) on the latent TB population (denoted as E) over a two-year period is illustrated. As smoking intensity increases from $\alpha = 0.55$ to $\alpha = 0.85$, there is a noticeable rise in the peak of the latent TB population, followed by a gradual decline. This suggests that higher smoking intensity leads to a larger latent TB population, potentially due to the immunosuppressive effects of smoking, which could increase susceptibility to TB infection and prolong the latent phase. This larger reservoir of latent TB cases poses a significant risk, as more individuals are likely to progress to the infectious stage, causing the spread of TB.

In the Figure 4b, the effect of different smoking-related transmission rates (β values) on the undetected active TB population (I_1) over the same two-year period is shown. Higher β values, indicating increased transmission due to smoking, result in a larger undetected active TB population. The graph shows that as β increases from 0.15 to 0.20, the peak of the undetected active TB population also increases and occurs later, with a more prolonged decline. This indicates that smoking not only accelerates TB transmission but also contributes to a larger pool of undetected active TB cases, potentially making the spread of the disease in the community. This larger undetected population indicates that smoking not only increases the likelihood of transmission but also complicates the detection and control of active TB cases. The combination of higher α and β due to smoking creates a scenario where TB spreads more rapidly and becomes harder to control, highlighting the need for targeted interventions to address smoking as a significant risk factor in TB transmission.

4. Application of optimal control

The spread of TB disease among smokers can be effectively controlled through various interventions. In this study, we employed three control measures aimed at curbing TB incidence within smoking populations. These controls include implementing social distancing measures (u_1) to reduce close contact and transmission, conducting targeted TB examinations (u_2) among populations at high risk of contracting TB, and providing essential TB treatment assistance (u_3) to disadvantaged communities with limited access to healthcare resources.

The mathematical model used to simulate the spread of TB disease among smokers with case detection incorporates these control variables. By integrating these measures into the model, we can assess their effectiveness in mitigating TB transmission and reducing the overall burden of the disease within the smoking population. The inclusion of control variables allows us to explore the impact of targeted interventions on disease dynamics and evaluate their potential for practical implementation in real-world settings.

The mathematical representation of the spread of TB disease among smokers with case detection, accompanied by the control variables, is as follows:

$$\frac{dS}{dt} = \varepsilon\Lambda - \alpha hS (I_1 + \gamma I_2) - (\mu + \kappa)S, \quad (4.1)$$

$$\frac{dM}{dt} = \Lambda - \varepsilon\Lambda - \alpha M (I_1 + \gamma I_2) (1 - u_1) - (\mu + \kappa)M, \quad (4.2)$$

$$\frac{dV}{dt} = \kappa(S + M) - \alpha(1 - \psi)V(I_1 + \gamma I_2) - \mu V, \quad (4.3)$$

$$\frac{dE}{dt} = \alpha (I_1 + \gamma I_2) (hS + M(1 - u_1) + (1 - \psi) V + \delta T) - (\tau + \beta + \mu) E, \quad (4.4)$$

$$\frac{dI_1}{dt} = (1 - \omega) \beta E - (\mu + d_1) I_1 - u_2 I_1, \quad (4.5)$$

$$\frac{dI_2}{dt} = \omega \beta E - (\mu + d_2 + r) I_2 + u_2 I_1 - u_3 I_2, \quad (4.6)$$

$$\frac{dT}{dt} = \tau E + r I_2 - \delta \alpha T (I_1 + \gamma I_2) - \mu T + u_3 I_2. \quad (4.7)$$

Through numerical simulations and sensitivity analyses, we can evaluate the effectiveness of each control measure in achieving our goal of minimizing TB incidence and improving public health outcomes among smoking populations. This comprehensive approach shows how the importance of different interventions in combating TB and demonstrates the significance of tailored strategies for vulnerable populations. The performance index of the mathematical model of the spread of TB disease among smokers with case detection accompanied by control variables is defined as follows:

$$\text{Min}J(u_1, u_2, u_3) = \int_0^{t_f} \left(A_1 E + A_2 I_1 + A_3 I_2 + \frac{c_1}{2} (u_1)^2 + \frac{c_2}{2} (u_2)^2 + \frac{c_3}{2} (u_3)^2 \right) dt,$$

where $0 \leq u_1, u_2, u_3 \leq 1$ and $A_1, A_2, A_3, c_1, c_2, c_3 > 0$. The coefficients c_1, c_2, c_3 and A_1, A_2, A_3 respectively are the weighting constants corresponding to each control and the weighting constants corresponding to the minimized population E, I_1 and I_2 . Optimal control time out is at an interval

$$t_0 \leq t \leq t_f$$

that expresses the time of observation made, which is the time when the control is given to the end time of the control. The quadratic function of the control cost is adopted, as stated in [28–30]. The term

$$\frac{c_1}{2} (u_1)^2 + \frac{c_2}{2} (u_2)^2 + \frac{c_3}{2} (u_3)^2$$

represents the costs associated with the TB prevention, TB treatment, and successful TB treatment controls, respectively.

Optimal control of the mathematical model of the spread of TB disease among smokers with case detection is completed using the Pontryagin maximum principle method. The Hamiltonian is obtained

$$\begin{aligned} H = & A_1 E + A_2 I_1 + A_3 I_2 + \frac{c_1}{2} u_1^2 + \frac{c_2}{2} u_2^2 + \frac{c_3}{2} u_3^2 \\ & + \lambda_1 (\varepsilon \Lambda - \alpha h S (I_1 + \gamma I_2) - (\mu + \kappa) S) \\ & + \lambda_2 (\Lambda - \varepsilon \Lambda - \alpha M (I_1 + \gamma I_2) (1 - u_1) - (\mu + \kappa) M) \\ & + \lambda_3 (\kappa (S + M) - \alpha (1 - \psi) V (I_1 + \gamma I_2) - \mu V) \\ & + \lambda_4 (\alpha (I_1 + \gamma I_2) (h S + M (1 - u_1) + (1 - \psi) V + \delta T) - (\tau + \beta + \mu) E) \\ & + \lambda_5 ((1 - \omega) \beta E - (\mu + d_1) I_1 - u_2 I_1) \\ & + \lambda_6 (\omega \beta E - (\mu + d_2 + r) I_2 + u_2 I_1 - u_3 I_2) \\ & + \lambda_7 (\tau E + r I_2 - \delta \alpha T (I_1 + \gamma I_2) - \mu T + u_3 I_2). \end{aligned}$$

Optimal conditions are obtained when the Hamiltonian function satisfies the following stationary conditions

$$\frac{\partial H}{\partial u_1} = 0, \quad \frac{\partial H}{\partial u_2} = 0, \quad \frac{\partial H}{\partial u_3} = 0.$$

So that the optimal controllers u_1, u_2 and u_3 are obtained

$$\begin{aligned} u_1^* &= \min \left(1, \max \left(0, \frac{\lambda_4 M (I_1 + \gamma I_2) - \lambda_2 \alpha M (I_1 + \gamma I_2)}{C_1} \right) \right), \\ u_2^* &= \min \left(1, \max \left(0, \frac{\lambda_5 I_1 - \lambda_6 I_1}{C_2} \right) \right), \\ u_3^* &= \min \left(1, \max \left(1, \frac{\lambda_7 I_2 - \lambda_6 I_2}{C_3} \right) \right). \end{aligned}$$

The state variables in u_1^* , u_2^* and u_3^* are obtained by solving the state equation

$$\dot{x} = \frac{\partial H}{\partial f},$$

while the Lagrange multiplier for the controls u_1^* , u_2^* and u_3^* is obtained by solving the Lagrange equation

$$\dot{x} = -\frac{\partial H}{\partial x}.$$

Then, the state variable and the Lagrange multiplier are substituted into u^* . The optimal solution from the mathematical model is determined by substituting the control u^* into the state equation.

The controller forms of u_1^* , u_2^* and u_3^* depend on state and costate variables. The state equations are as follows:

$$\begin{aligned} \frac{dS}{dt} &= \frac{\partial H}{\partial f_1} = \varepsilon \Lambda - \alpha h S (I_1 + \gamma I_2) - (\mu + \kappa) S, \\ \frac{dM}{dt} &= \frac{\partial H}{\partial f_2} = \Lambda - \varepsilon \Lambda - \alpha M (I_1 + \gamma I_2) (1 - u_1) - (\mu + \kappa) M, \\ \frac{dV}{dt} &= \frac{\partial H}{\partial f_3} = \kappa (S + M) - \alpha (1 - \psi) V (I_1 + \gamma I_2) - \mu V, \\ \frac{dE}{dt} &= \frac{\partial H}{\partial f_4} = \alpha (I_1 + \gamma I_2) (h S + M (1 - u_1) + (1 - \psi) V + \delta T) - (\tau + \beta + \mu) E, \\ \frac{dI_1}{dt} &= \frac{\partial H}{\partial f_5} = (1 - \omega) \beta E - (\mu + d_1) I_1 - u_2 I_1, \\ \frac{dI_2}{dt} &= \frac{\partial H}{\partial f_6} = \omega \beta E - (\mu + d_2 + r) I_2 + u_2 I_1 - u_3 I_2, \\ \frac{dT}{dt} &= \frac{\partial H}{\partial f_7} = \tau E + r I_2 - \delta \alpha T (I_1 + \gamma I_2) - \mu T + u_3 I_2. \end{aligned} \tag{4.8}$$

Meanwhile, the costate equations are as follows:

$$\dot{\lambda}_1 = -\frac{\partial H}{\partial S} = \lambda_2 \alpha ((I_1 + \gamma I_2) (1 - u_1) + \mu + \kappa) - \lambda_3 \kappa - \lambda_4 \alpha (I_1 + \gamma I_2) (1 - u_1),$$

$$\begin{aligned}
\dot{\lambda}_2 &= -\frac{\partial H}{\partial M} = \lambda_2\alpha((I_1 + \gamma I_2)(1 - u_1) + \mu + \kappa) - \lambda_3\kappa - \lambda_4\alpha(I_1 + \gamma I_2)(1 - u_1), \\
\dot{\lambda}_3 &= -\frac{\partial H}{\partial V} = \lambda_3(\alpha(1 - \psi)(I_1 + \gamma I_2) + \mu) - \lambda_4\alpha(I_1 + \gamma I_2)(1 - \psi), \\
\dot{\lambda}_4 &= -\frac{\partial H}{\partial E} = -A_1 + \lambda_4(\tau + \beta + \mu) - \lambda_5(1 - \omega)\beta - \lambda_6\omega\beta - \lambda_7\tau, \\
\dot{\lambda}_5 &= -\frac{\partial H}{\partial I_1} = -A_2 + \lambda_1\alpha hS + \lambda_2\alpha M(1 - u_1) + \lambda_3\alpha(1 - \psi)V \\
&\quad - \lambda_4\alpha(hS + M(1 - u_1) + (1 - \psi)V + \delta T) + \lambda_5(\mu + d_1 + u_2) - \lambda_6u_2, \\
\dot{\lambda}_6 &= -\frac{\partial H}{\partial I_2} = \lambda_1\alpha hS\gamma + \lambda_2\alpha M\gamma(1 - u_1) + \lambda_3\alpha(1 - \psi)V\gamma + \lambda_6(\mu + d_2 + r + u_3) \\
&\quad - \lambda_4\alpha\gamma(hS + M(1 - u_1) + (1 - \psi)V + \delta T) - \lambda_7(r + u_3) + \lambda_7\delta\alpha T\gamma, \\
\dot{\lambda}_7 &= -\frac{\partial H}{\partial T} = -\lambda_4\alpha(I_1 + \gamma I_2)\delta + \lambda_7\delta\alpha(I_1 + \gamma I_2) + \lambda_7\mu.
\end{aligned} \tag{4.9}$$

Based on the description above, to get the values of S , M , V , E , I_1 , I_2 , and T from the optimal form u_1^* , u_2^* , and u_3^* , it is necessary to solve the nonlinear state and costate equations. The nonlinear equation system is hard to be solved analytically, so the solutions to the equation of state are analyzed using numerical simulations.

5. Numerical results

The state equation in the numerical simulation program for the mathematical model of the spread of TB disease among smokers with case detection is defined as

$$S = y(1), M = y(2), V = y(3), E = y(4), I_1 = y(5), I_2 = y(6) \text{ and } T = y(7).$$

The performance index is defined as a new state equation that is $J = y(8)$ and controls u_1 , u_2 and u_3 are defined as $u(1)$, $u(2)$ dan $u(3)$. The simulation is carried out using initial values, namely

$$S(t_0) = 16, M(t_0) = 20, V(t_0) = 30, E(t_0) = 35, I_1(t_0) = 11, I_2(t_0) = 10 \text{ and } T(t_0) = 9$$

with the start and end times, respectively, as $t_0 = 0$ and $t_f = 2$ in years. Defined weighting constants to minimize the population (A) and the costs needed to apply each control (c), respectively, are

$$A_1 = 1, A_2 = 1, A_3 = 1, c_1 = 1, c_2 = 1 \text{ and } c_3 = 1.$$

They have been standardized to 1 for the purpose of simplifying the calculations. This normalization allows for a more straightforward analysis by eliminating the variability introduced by differing cost magnitudes, thus focusing the analysis on the structural or relative relationships within the model.

This research distinguishes itself by directly integrating smoking behavior into the mathematical modeling of TB transmission. By centering smoking habits in the transmission dynamics, our model provides a more accurate representation of high-risk populations where smoking is common. This approach enables the identification of targeted control strategies, such as social distancing among smokers and tailored TB screening and treatment, guided by optimal control theory to find the most

effective interventions. The improved outcomes come from directly addressing the significant role of smoking in TB spread, offering a comprehensive framework for disease control in smoking-heavy populations.

The optimal control simulations of TB spread among smokers with case detection highlight the effectiveness of intervention strategies compared to scenarios without controls. Figure 5a illustrates that control strategies u_1 and u_2 exhibit the most significant impact on reducing the number of latent TB cases compared to other control strategies. This finding underscores the effectiveness of interventions focused on social distancing (u_1) and targeted TB examinations (u_2) in curbing TB transmission and preventing the progression of latent TB to active disease within the smoking population. While control strategies involving u_1 and u_3 as well as u_1, u_2 and u_3 also demonstrate notable effectiveness in reducing the number of latent TB cases, their impact is not as pronounced as that of u_1 and u_2 strategies alone. This suggests that while providing TB treatment assistance (u_3) is beneficial, its effect on reducing latent TB cases may be less noticeable by the more targeted interventions of social distancing and TB examinations.

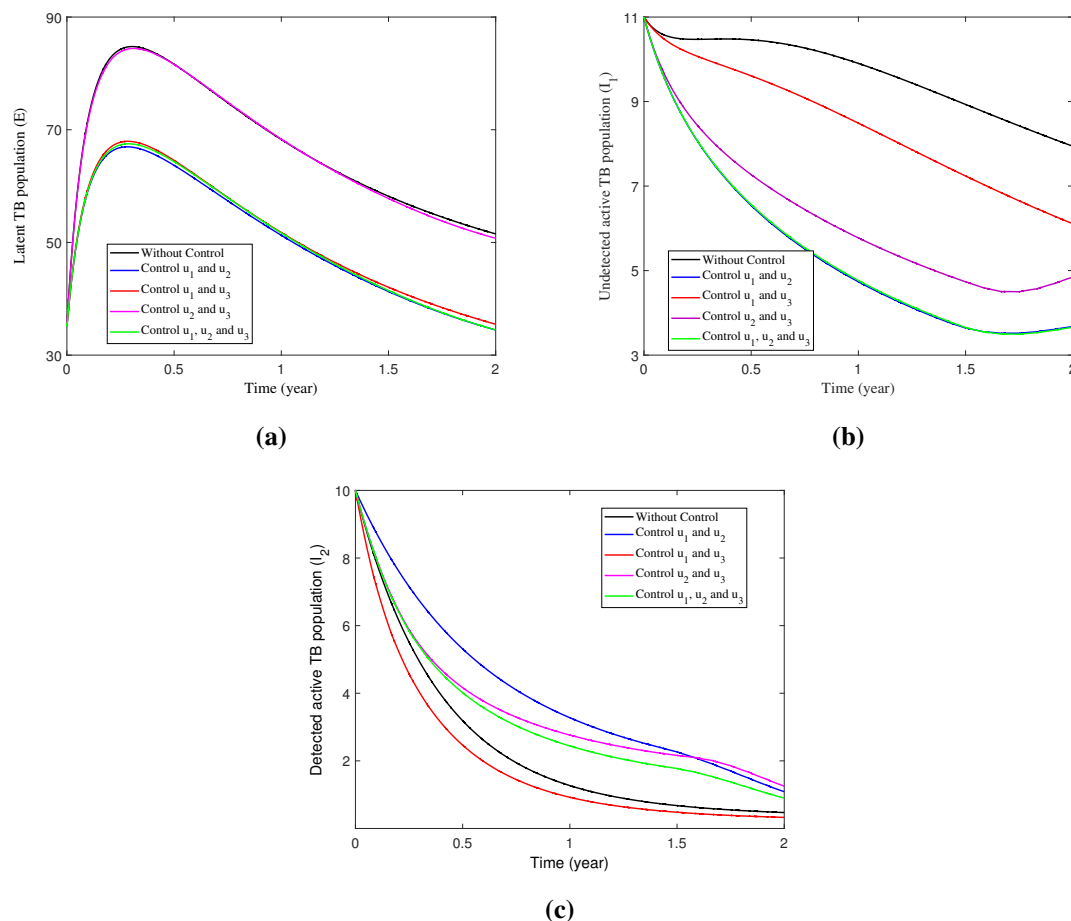


Figure 5. Comparison between the number population (a) exposed, (b) undetected active TB, and (c) detected active TB population without and with control. All parameter values are in Table 2.

Figure 5b demonstrates that control strategies u_1, u_2 and u_3 have the most significant impact on

reducing the number of undetected active TB cases. This finding underscores the crucial role of interventions such as social distancing, targeted TB examinations, and TB treatment assistance in effectively identifying and managing active TB cases within the smoking population. The reduction in the number of undetected active TB cases is particularly significant as it leads to an increase in the TB CDR. A higher CDR facilitates earlier detection and treatment of TB cases, thereby preventing further transmission of the disease within the community. By effectively identifying and treating active TB cases, public health authorities can mitigate the spread of TB and reduce the overall burden of the disease on the population. While control strategies involving u_1 and u_2 also demonstrate substantial effectiveness in reducing the number of undetected active TB patients, their impact is not as pronounced as that of the combined strategies including u_1 , u_2 and u_3 . This suggests that while social distancing and targeted examinations play crucial roles in TB control, the addition of TB treatment assistance further enhances the effectiveness of control efforts, particularly in reducing undetected active TB cases.

Figure 5c shows that the implementation of control strategies u_1 and u_3 together results in a significant reduction in the number of detected active TB cases. By simultaneously reducing TB transmission through social distancing and ensuring prompt treatment for active cases, this combined approach proves highly effective in limiting the number of individuals suffering from active TB.

The optimal control strategies applied to the TB model demonstrate a significant reduction in the latent, undetected active, and detected active TB populations over time. However, none of these populations reach zero by the end of the simulation period. This outcome can be attributed to several biological and epidemiological factors.

Complete eradication may not occur due to limited reach or adherence to control measures. Some individuals may not fully comply with treatment programs or preventive strategies, allowing latent or undetected infections to persist. In particular, latent TB infections (as shown in Figure 5a) are challenging to eliminate entirely, as individuals with latent TB remain asymptomatic for long periods. These individuals can also re-enter the infectious population if their immune system weakens over time.

Figure 5b highlights the persistence of undetected active TB despite the application of control interventions, indicating gaps in detection efforts. Some individuals may remain undiagnosed due to barriers such as limited access to healthcare services or social stigma, which hinder comprehensive control. Additionally, epidemiological control strategies often encounter diminishing returns; as the infected population decreases to low levels, the effort required to reduce it further becomes increasingly demanding, leading to a plateau in progress before eradication can be achieved.

The persistence of low-level TB populations, even under optimal control strategies, aligns with findings from previous studies. Research suggests that TB elimination is inherently difficult due to the disease's biological complexity, the nature of latent infections, and social challenges in implementing control measures effectively [31]. Moreover, mathematical models in infectious disease dynamics emphasize that complete eradication requires not only robust control strategies but also broader societal efforts, such as improved living conditions and strengthened public health infrastructure [32].

To further illustrate the comparative effectiveness of each control strategy, Table 5 presents a comparison of the number of patients with latent TB and active TB at the end of the observation period for each strategy. This analysis provides valuable insights into the relative impact of different interventions on TB transmission dynamics and disease burden within the smoking population.

Table 5. Comparison of the number of TB sufferers at the end of the observation E, I_1, I_2 with and without control.

| Condition | Total population (end of observation) | | | Total TB patients | Cost value |
|------------------------------|---------------------------------------|--------|--------|-------------------|------------|
| | E | I_1 | I_2 | | |
| No control | 51.5098 | 7.9431 | 0.4710 | 59.9239 | - |
| Control u_1 and u_2 | 34.4523 | 3.6763 | 1.0884 | 39.2170 | 122.1529 |
| Control u_1 and u_3 | 35.4740 | 6.1091 | 0.3281 | 41.9112 | 124.8652 |
| Control u_2 and u_3 | 50.7343 | 4.8474 | 1.2525 | 56.8342 | 155.0391 |
| Control u_1, u_2 and u_3 | 34.4694 | 3.6578 | 0.8980 | 39.0252 | 121.6200 |

The implementation of control strategies u_1 and u_2 yields a substantial reduction in the number of TB sufferers by 34.55%. Further analysis reveals that employing control strategies u_1 and u_3 , as well as u_2 and u_3 respectively, can minimize the number of TB patients by 30.06% and 5.16%. Remarkably, the combined implementation of control strategies u_1, u_2 and u_3 achieves the highest reduction, minimizing TB sufferers by 37.87%. These findings indicate that the comprehensive approach of implementing all three control strategies simultaneously is the most effective strategy in minimizing the number of TB sufferers.

Furthermore, beyond their effectiveness, it is essential to consider the cost implications of each control strategy. The associated costs for implementing these strategies are detailed in Table 5. The simultaneous application of the three controls u_1, u_2 , and u_3 has the most significant impact in reducing the number of TB patients compared to other control strategies. This strategy also results in the most favorable cost values. To achieve optimal outcomes with minimal cost, the recommended strategy involves implementing control u_1 at 100% effort for two years, control u_2 at 100% effort for 18 months, and control u_3 at 100% effort for two months.

The effort percentage for controls u_2 and u_3 gradually decreases starting from the 19th month and the third month, respectively, until the end of the observation period at month 24. The required cost for implementing this strategy is illustrated in Figure 6. By carefully adjusting the level of control effort during each specific period, optimal results can be achieved, both in terms of reducing the infected population and minimizing cost.

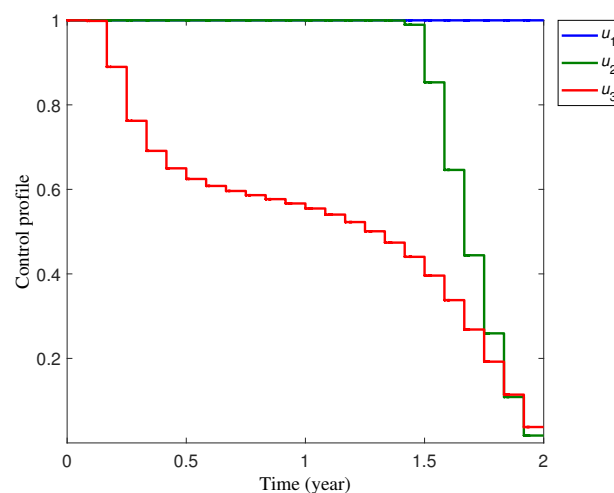


Figure 6. Graph u_1, u_2 and u_3 control profiles.

Considering both effectiveness and cost, the strategy of implementing controls u_1, u_2 and u_3 emerges as the optimal approach, striking a favorable balance between minimizing the number of TB cases and maximizing the efficient use of resources. This highlights the critical importance of adopting comprehensive, cost-effective control measures to effectively address TB, particularly within vulnerable groups such as smokers. By combining multiple interventions, policy makers and public health officials can optimize TB control efforts, leading to improved health outcomes and reduced TB burden within vulnerable populations like smokers.

6. Conclusions

In this paper, we have analyzed a model of TB spread within a population of smokers, considering the case detection rate. Our model identifies two types of equilibrium: non-endemic and endemic. The non-endemic equilibrium is locally asymptotically stable when the basic reproduction number (R_0) is less than one. To further understand the dynamics of TB spread, we conducted a parameter sensitivity analysis to identify which parameters most significantly influence disease transmission. Notably, we found that the rate of progression from latent TB to active TB and the TB transmission rate are critical parameters that significantly impact the value of R_0 . These parameters play a crucial role in determining the potential for an outbreak and the overall stability of the disease within the population.

This paper's key innovation lies in integrating smoking behavior as a pivotal factor in TB transmission dynamics. This approach provides a more comprehensive understanding of TB spread among smokers and highlights the unique challenges faced by this vulnerable group. Additionally, we explored optimal control strategies, including implementing social distancing among smokers, conducting TB examinations for high-risk populations, and providing TB treatment to low-income communities. Our findings suggest that these interventions are both effective and efficient in reducing the number of TB cases, especially when considering associated costs. By focusing on the most influential parameters and applying targeted interventions, we can better manage and reduce TB transmission.

However, this study has some limitations. Our model assumes constant parameter values and does not account for possible time-dependent variations or delays in TB progression and detection. Additionally, while we incorporated smoking behavior, other factors such as coinfection with other diseases, varying socioeconomic conditions, and environmental influences were not included. These factors could further refine the model and enhance its predictive power.

As a next step, we propose modifying the current model into a fractional-order model [12, 16, 33]. Fractional models have been shown to provide a more accurate representation of real-world dynamics due to their ability to capture memory effects and anomalous diffusion processes, which are prevalent in biological systems. This approach can offer a more nuanced understanding of TB spread, especially in populations with complex behavior patterns like smokers. By incorporating fractional derivatives, the model can account for the long-term impact of past behaviors on current infection dynamics, potentially leading to more precise predictions and more effective control strategies.

Future work will also involve expanding the model to include additional risk factors, refining parameter estimations with real-world data, and exploring the combined impact of multiple intervention strategies in a more holistic framework. These improvements aim to enhance the applicability of our model in public health planning and policy-making, ensuring that resources are

utilized in the most impactful manner to curb TB spread among vulnerable populations.

Author contributions

Cicik Alfiniyah: conceptualization, original draft preparation, supervision, validation of results, formal analysis, investigation, writing and review; Wanwha Sonia Putri Artha Soetjianto: methodology, project administration, software development, investigation; Ahmadin: methodology, writing and review; Muhamad Hifzhudin Noor Aziz: software development, validation of results, investigation; Siti Maisharah Sheikh Ghadz: formal analysis. All authors have reviewed and approved the final version for publication.

Acknowledgments

This research was funded by SATU Joint Research Schema (JRS), Universitas Airlangga, Indonesia (grant number: 1600/UN3.LPPM/PT.01.03/2023).

Conflict of interest

The authors declare no conflicts of interest.

References

1. R. Miggiano, M. Rizzi, D. M. Ferraris, Mycobacterium tuberculosis pathogenesis, infection prevention and treatment, *Pathogens*, **9** (2020), 385. <https://doi.org/10.3390/pathogens9050385>
2. A. Selmani, M. Coenen, S. Voss, C. Jung-Sievers, Health indices for the evaluation and monitoring of health in children and adolescents in prevention and health promotion: a scoping review, *BMC Public Health*, **21** (2021), 2309. <https://doi.org/10.1186/s12889-021-12335-x>
3. B. Mathema, J. R. Andrews, T. Cohen, M. W. Borgdorff, M. Behr, J. R. Glynn, et al., Drivers of tuberculosis transmission, *J. Infect. Dis.*, **216** (2017), S644–S653. <https://doi.org/10.1093/infdis/jix354>
4. S. Kiazzyk, T. B. Ball, Latent tuberculosis infection: an overview, *Can. Commun. Dis. Rep.*, **43** (2017), 62–66. <https://doi.org/10.14745/ccdr.v43i34a01>
5. M. Farman, C. Alfiniyah, A. Shehzad, Modelling and analysis tuberculosis (TB) model with hybrid fractional operator, *Alex. Eng. J.*, **72** (2023), 463–478. <https://doi.org/10.1016/j.aej.2023.04.017>
6. Fatmawati, U. D. Purwati, M. I. Utoyo, C. Alfiniyah, Y. Prihartini, The dynamics of tuberculosis transmission with optimal control analysis in Indonesia, *Commun. Math. Biol. Neurosci.*, **2020** (2020), 25. <https://doi.org/10.28919/cmbn/4605>
7. T. Fanirana, A. Alib, M. O. Adewolec, B. Adebod, O. O. Akannie, Asymptotic behavior of Tuberculosis between smokers and non-smokers, *Partial Differ. Equations Appl. Math.*, **5** (2022), 100244. <https://doi.org/10.1016/j.padiff.2021.100244>

8. K. Slama, C. Y. Chiang, D. A. Enaderson, K. Hasmler, A. Fanning, P. Gupta, et al., Tobacco and tuberculosis: a qualitative systematic review and meta-analysis, *Int. J. Tuberc. Lung Dis.*, **11** (2007), 1049–1061.
9. D. Gao, N. Huang, Optimal control analysis of a tuberculosis model, *Appl. Math. Modell.*, **58** (2018), 47–64. <https://doi.org/10.1016/j.apm.2017.12.027>
10. A. Y. Ayinla, W. A. M. Othman, M. Rabiou, A mathematical model of the tuberculosis epidemic, *Acta Biotheor.*, **69** (2021), 225–255. <https://doi.org/10.1007/s10441-020-09406-8>
11. S. Basu, D. Stuckler, A. Bitton, S. A. Glantz, Projected effects of tobacco smoking on worldwide tuberculosis control: mathematical modeling analysis, *BMJ*, **4** (2011), 343. <https://doi.org/10.1136/bmj.d5506>
12. Fatmawati, M. A. Khan, E. Bonyah, Z. Hammouch, E. M. Shaiful, A mathematical model of tuberculosis (TB) transmission with children and adults groups: a fractional model, *AIMS Math.*, **5** (2020), 2813–2842. <https://doi.org/10.3934/math.2020181>
13. C. P. Bhunu, Mathematical analysis of a three-strain tuberculosis transmission model, *Appl. Math. Model.*, **35** (2011), 4647–4660. <https://doi.org/10.1016/J.APM.2011.03.037>
14. J. J. Tewa, S. Bowong, B. Mewoli, Mathematical analysis of two-patch model for the dynamical transmission of tuberculosis, *Appl. Math. Model.*, **36** (2012), 2466–2485. <https://doi.org/10.1016/J.APM.2011.09.004>
15. J. Liu, T. Zhang, Global stability for a tuberculosis model, *Math. Comput. Model.*, **54** (2011), 836–845. <https://doi.org/10.1016/j.mcm.2011.03.033>
16. S. Ullah, M. A. Khan, M. Farooq, A fractional model for the dynamics of TB virus, *Chaos Solitons Fract.*, **116** (2018), 63–71. <https://doi.org/10.1016/j.chaos.2018.09.001>
17. M. A. Khan, M. Ahmad, S. Ullah, M. Farooq, T. Gul, Modeling the transmission dynamics of tuberculosis in Khyber Pakhtunkhwa Pakistan, *Adv. Mech. Eng.*, **11** (2019), 1–13. <https://doi.org/10.1177/1687814019854835>
18. F. B. Augusto, Optimal chemoprophylaxis and treatment control strategies of a tuberculosis transmission model, *World J. Model. Simul.*, **5** (2009), 163–173.
19. C. J. Silva, D. F. M. Torres, Optimal control for a tuberculosis model with reinfection and post-exposure interventions, *Math. Biosci.*, **244** (2013), 154–164. <https://doi.org/10.1016/j.mbs.2013.05.005>
20. P. Rodrigues, C. J. Silva, D. F. M. Torres, Cost-effectiveness analysis of optimal control measures for tuberculosis, *Bull. Math. Bio.*, **76** (2014), 2627–2645. <https://doi.org/10.1007/s11538-014-0028-6>
21. D. Okuonghae, Analysis of stochastic mathematical model for tuberculosis with case detection, *Int. J. Dyn. Control*, **10** (2022), 734–747. <https://doi.org/10.1007/s40435-021-00863-8>
22. O. Diekmann, J. A. P. Heesterbeek, J. A. J. Metz, On the definition and the computation of the basic reproduction ratio R_0 in models for infectious diseases in heterogenous populations, *J. Math. Biol.*, **28** (1990), 362–382. <https://doi.org/10.1007/BF00178324>
23. O. Diekmann, J. A. P. Heesterbeek, *Mathematical epidemiology of infectious diseases: model building, analysis and interpretation*, John Wiley & Sons, Inc., 2000.

24. P. van den Driessche, J. Watmough, Reproduction numbers and sub-threshold endemic equilibria for compartmental models of disease transmission, *Math. Biosci.*, **180** (2002), 29–48. [https://doi.org/10.1016/S0025-5564\(02\)00108-6](https://doi.org/10.1016/S0025-5564(02)00108-6)
25. H. Abboubakar, J. C. Kamgang, L. N. Nkamba, D. Tieudjo, Bifurcation thresholds and optimal control in transmission dynamics of arboviral diseases, *J. Math. Biol.*, **76** (2018), 379–427. <https://doi.org/10.1007/s00285-017-1146-1>
26. L. N. Nkamba, T. T. Manga, F. Agouanet, M. L. M. Manyombe, Mathematical model to assess vaccination and effective contact rate impact in the spread of tuberculosis, *J. Biol. Dyn.*, **13** (2019), 26–42. <https://doi.org/10.1080/17513758.2018.1563218>
27. N. Chitnis, J. M. Hyman, J. M. Cushing, Determining important parameters in the spread of malaria through the sensitivity analysis of a mathematical model, *Bull. Math. Biol.*, **70** (2008), 1272–1296. <https://doi.org/10.1007/s11538-008-9299-0>
28. K. O. Okosun, O. D. Makinde, A co-infection model of malaria and cholera diseases with optimal control, *Math. Biosci.*, **258** (2014), 19–32. <https://doi.org/10.1016/j.mbs.2014.09.008>
29. K. O. Okosun, O. D. Makinde, Optimal control analysis of hepatitis C virus with acute and chronic stages in the presence of treatment and infected immigrants, *Int. J. Biomath.*, **7** (2014), 1450019. <https://doi.org/10.1142/S1793524514500193>
30. G. T. Tilahun, O. D. Makinde, D. Malonza, Co-dynamics of pneumonia and typhoid fever diseases with cost effective optimal control analysis, *Appl. Math. Comput.*, **316** (2018), 438–459. <https://doi.org/10.1016/j.amc.2017.07.063>
31. E. Ziv, C. L. Daley, S. Blower, Early therapy for latent tuberculosis infection, *Am. J. Epidemiol.*, **153** (2001), 381–385. <https://doi.org/10.1093/aje/153.4.381>
32. E. Vynnycky, P. E. Fine, The natural history of tuberculosis: the implications of age-dependent risks of disease and the role of reinfection, *Epidemiol. Infect.*, **119** (1997), 183–201. <https://doi.org/10.1017/s0950268897007917>
33. K. Hattaf, A new mixed fractional derivative with applications in computational biology, *Computation*, **12** (2024), 7. <https://doi.org/10.3390/computation12010007>



AIMS Press

©2024 the Author(s), licensee AIMS Press. This is an open access article distributed under the terms of the Creative Commons Attribution License (<https://creativecommons.org/licenses/by/4.0>)